Available online at www.sciencedirect.com
ScienceDirect
Journal of Molecular Graphics and Modelling 26 (2007) 62–68
Journal of Molecular Graphics and Modelling
www.elsevier.com/locate/JMGM

Molecular dynamics analysis of HIV-1 matrix protein: Clarifying differences between crystallographic and solution structures

Hugo Verli [a,b,*], Alexandre Calazans [c], Rodrigo Brindeiro [c], Amilcar Tanuri [c], Jorge A. Guimarães [b]

[a] Faculdade de Farmácia, Universidade Federal do Rio Grande do Sul, Av. Ipiranga, 2752, Porto Alegre 90610-000, RS, Brazil
[b] Centro de Biotecnologia, Univerdade Federal do Rio Grande do Sul, Av. Bento Gonçalves, 9500, CP 15005, Porto Alegre 91500-970, RS, Brazil
[c] Departmento de Genética, Instituto de Biologia, Universidade Federal do Rio de Janeiro, RJ 21944-970, Brazil

Received 19 June 2006; received in revised form 12 September 2006; accepted 20 September 2006
Available online 26 September 2006

Abstract

One of the main structural features of the mature HIV-1 virion is the matrix protein (p17). This partially globular protein presents four helixes centrally organized and a fifth one, H5, projecting away from the packed bundle of helixes. Comparison between solution and crystallographic data of p17 indicates a 6 Å displacement of a short 3_{10} helix and a partial unfolding of H5 in solution related to crystal. While the behavior of the 3_{10} helix has been previously addressed to virion assembly, the relevance and origin of H5 partial unfolding is possibly related to the contacts between p17 and other viral elements, such as p24. In this context, we present a 40 ns conformational sampling of monomeric p17 using molecular dynamics simulations. The performed simulations presented a progressive conversion of the p17 crystallographic structure to the NMR conformation, suggesting that the biological form of this protein may have its C-terminal portion partially unfolded.

Keywords: Molecular dynamics; HIV-1 matrix protein; Crystallographic contacts; p17; p24

1. Introduction

The structural features of the mature HIV-1 virion include a lipid bilayer envelope, surface glycoproteins (gp120) anchored to the virus through interactions with a transmembrane protein (gp41), a matrix shell (p17), and a conical capsid core (p24). In addition, two copies of the unspliced viral genome, stabilized by the nucleocapsid protein (p7), occur in the center of the virus together with viral enzymes (protease, reverse transcriptase and integrase) and accessory proteins (Nef, Vif, and Vpr) [1]. While a considerable amount of information is already known about these components in its isolated forms [1–9], the arrangement of such molecules to build the mature HIV-1 virion is, so far, not completely elucidated [10].

The HIV-1 matrix protein (p17) is a structural molecule, partially globular, composed by five α-helices (Fig. 1). The helixes H1, H2 and H3 are organized around the central and buried H4 [5], while H5 is projected from the packed helical bundle, making the C-terminal region of the protein distinct from its globular N-terminal (Fig. 2A). Additional elements on the secondary structure of this protein include the 3_{10}-helix H2′ and the mixed $\alpha/3_{10}$-helix H3′ [5].

Current data, based on crystallographic experiments [5], electron microscopy observations [3,7], and docking calculations [11] point to a trimeric organization of p17 monomers in the mature virion. Such organization appears to be also used by others HIV-1 structural proteins [10], in an organization defined by the Gag precursor. On the other hand, the precise contacts occurring between p17 and p24 remains poorly resolved [10].

One necessary step to resolve such contacts includes the precise elucidation of the three-dimensional structures of p17 and p24. Although there are currently several structural data of these molecules [2,4–6,12], some structural aspects of these proteins emerge from comparison between its solution and crystallographic forms. In fact, previous studies had reported a

* Corresponding author at: Faculdade de Farmácia, Universidade Federal do Rio Grande do Sul, Av. Ipiranga, 2752, Porto Alegre 90610-000, RS, Brazil. Tel.: +55 51 3316 7770; fax: +55 51 3316 7309.
E-mail address: hverli@cbiot.ufrgs.br (H. Verli).

1093-3263/$ – see front matter © 2006 Elsevier Inc. All rights reserved.
doi:10.1016/j.jmgm.2006.09.009

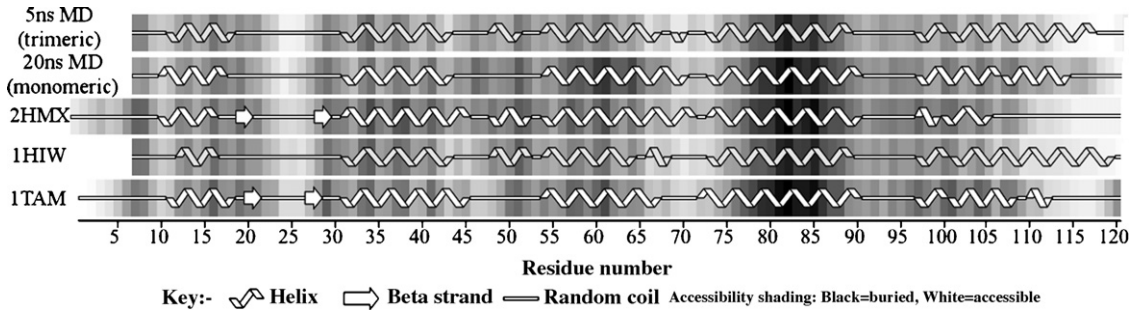

Fig. 1. Comparative description of p17 structure, obtained from different methodologies: crystal (PDB ID 1HIW), NMR (PDB ID 1TAM and 2HMX), and molecular dynamics simulation (5 ns under trimeric organization and 20 ns under the monomeric protein). Secondary structure was assigned using the PROCHECK program [18], comprising five α-helixes (H1–H5), a 3_{10} helixes (H2′, observed in 2HMX and 1HIW) and a mixed $\alpha/3_{10}$ helix (H3′, observed only in 1HIW).

6 Å displacement of the short helix H3′ when comparing X-ray and NMR structures [6]. Such displacement was interpreted by the authors as a physiologically relevant conformational change that occurs during virion assembly and disassembly. Additionally, the comparison of X-ray and NMR structures of p17 indicates an environment-dependent folding of the C-terminal helix H5. In solution, this α-helix is two turns shorter than in crystal, corresponding to an unfolding of more than seven amino acid residues [4] (Fig. 1). Considering that p17 interaction with the subjacent capsid depends on H5 conformation, we present in the current work a molecular dynamics study of p17 crystallographic structure. Our results elucidate the molecular basis for the differences between X-ray and NMR structures of HIV-1 matrix protein and, in the context of the molecular assembly of HIV-1 Gag proteins, may have relevant implications in the determinants of virion behavior during cellular infection at the atomic level.

2. Methods

2.1. Software

All simulations were performed using the GROMACS simulation suite and force field [13,14]. The Swiss-PDB Viewer [15], DSSP [16], STRIDE [17], and PROCHECK [18] programs were used in protein analyses, while PyMOL [19] was used for molecule visualization.

2.2. MD simulations of p17

The crystallographic structure of p17 was retrieved from Protein Data Bank under code 1HIW. This structure contains six monomers (chains A, B, C, Q, R and S) of the HIV-1 matrix protein, from which the protein A was used for the simulations. This molecule was solvated in a rectangular box using periodic

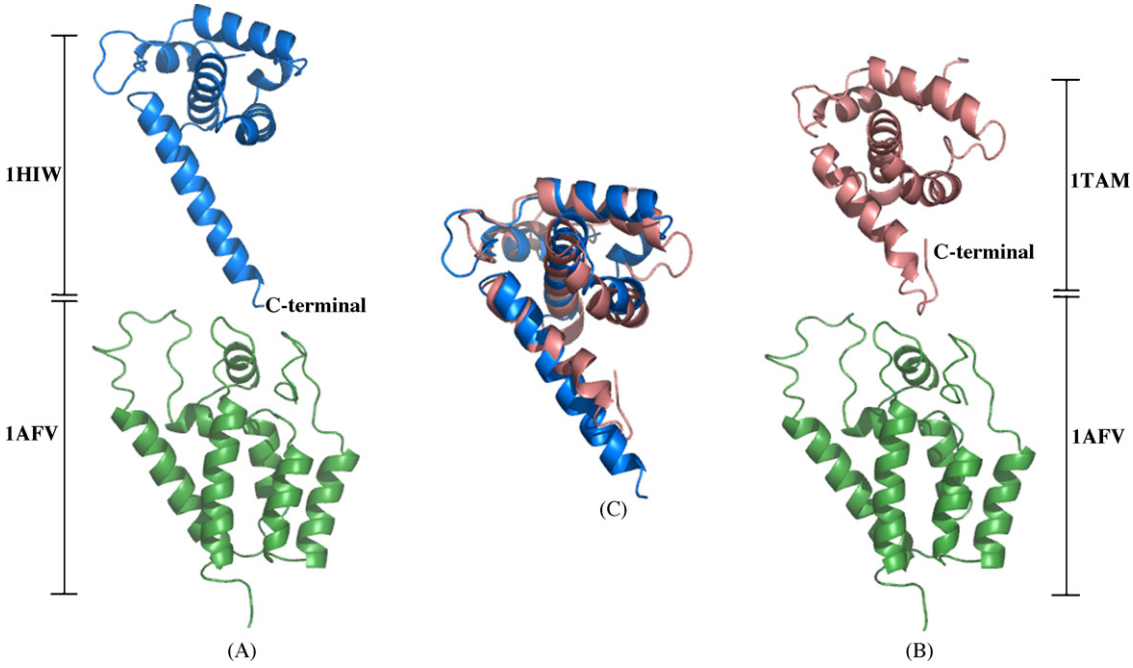

Fig. 2. Hypothetical organization between p17 and p24 (PDB ID 1AFV): (A) crystallographic conformation of p17 (PDB ID 1HIW); (B) solution conformation of p17 (PDB ID 1TAM); (C) superimposition of crystal and solution conformations of p17, emphasizing the different folding between the two conformations at the C-terminal helix (H5).

boundary conditions and SPC water model [20]. Counter ions were added to neutralize the system. The employed MD protocol was based on previous MD studies [21]. The Lincs and Settle methods [22,23] were applied to constrain covalent bond lengths, allowing an integration step of 2 fs after an initial energy minimization using Steepest Descents algorithm. Electrostatic interactions were calculated with particle mesh Ewald (PME) [24] and generalized reaction field (GRF) [25]. Temperature and pressure were kept constant by separately coupling the protein, ions, and solvent to external temperature and pressure baths [26], with coupling constants of $\tau = 0.1$ and 0.5 ps, respectively. The dielectric constant was treated as $\varepsilon = 1$, and the reference temperature was adjusted to 310 K. The system was slowly heated from 50 to 310 K, in steps of 5 ps, each one increasing the reference temperature by 50 K. Three simulations were performed, two using PME (one of 10 ns and one of 20 ns simulation) and one using GRF (a 10 ns simulation), totalizing 40 ns of conformational sampling of monomeric p17. Additional simulations were also performed with the trimeric p17, with a sampling time of 5 ns.

3. Results and discussion

3.1. Simulation stability

In order to monitor the progress of p17 conformational changes in MD and check the stability of its secondary structure elements, we evaluated the root mean square deviation (RMSD) for the simulated protein using as reference the crystallographic structure. As can be observed in Fig. 3A (black), the simulation was stable up to 10 ns, with a 0.3 nm average RMSD for the entire protein. After this period, the deviation from crystal structure significantly increases to about 0.5 nm. Since the main conformational difference between X-ray and NMR structures lie in the H5 helix, the RMSD for this C-terminal element is also presented in Fig. 3A (blue), as well as the deviation of p17 without H5 (red). These data clearly indicate that the origin of the high deviation from crystal structure in the last 10 ns of the simulation is due to conformational changes in H5, but not to distortions in the globular part of the matrix protein. The distortion in H5 during the second half of the simulation is correlated with a decrease in the radius of gyration (Fig. 3B, black), a modification not related to the globular part of p17 (Fig. 3B, red). Such results suggest a compacting process of the protein moiety in solution, mainly at the H5 helix.

The process of conformational modification of p17 occurs without major modification in physical–chemical properties of the protein, as the interaction energy between p17 and the surrounding solvent does not show meaningful changes in the trajectory (Fig. 3C). Moreover, there is a small lowering in the solvent-accessible surface (Fig. 3D), probably associated with the protein compacting process and, consequently, the lowering in H5 exposure to solvent.

3.2. Structural fluctuations of p17

While the data present in Fig. 3 gives a global perspective of the protein modifications over the MD trajectory, it lacks resolution at a residue level. To overcome this methodological simplification we used a strategy that describes the fluctuation of protein structure as a function of both time and residue number [27]. Applying this procedure, the analysis of RMSD from crystal structure (Fig. 4A) complemented the data of Fig. 3A, showing that, in fact, the main region of the protein

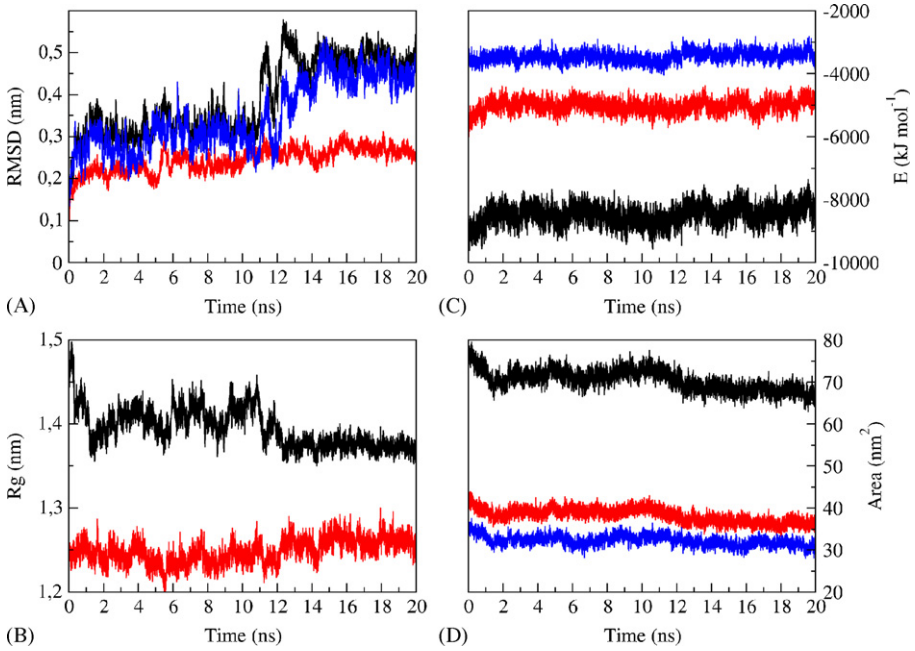

Fig. 3. (A) All-atom RMSD from crystal structure for entire p17 (black), for H5 (blue), and for p17 without H5 (red); (B) radius of gyration for entire p17 (black) and for p17 without H5 (red); (C) interaction energy between solvent and entire p17 (black), H5 (blue), and p17 without H5 (red); (D) total (black), hydrophobic (red), and hydrophilic (blue) solvent-accessible surfaces [35].

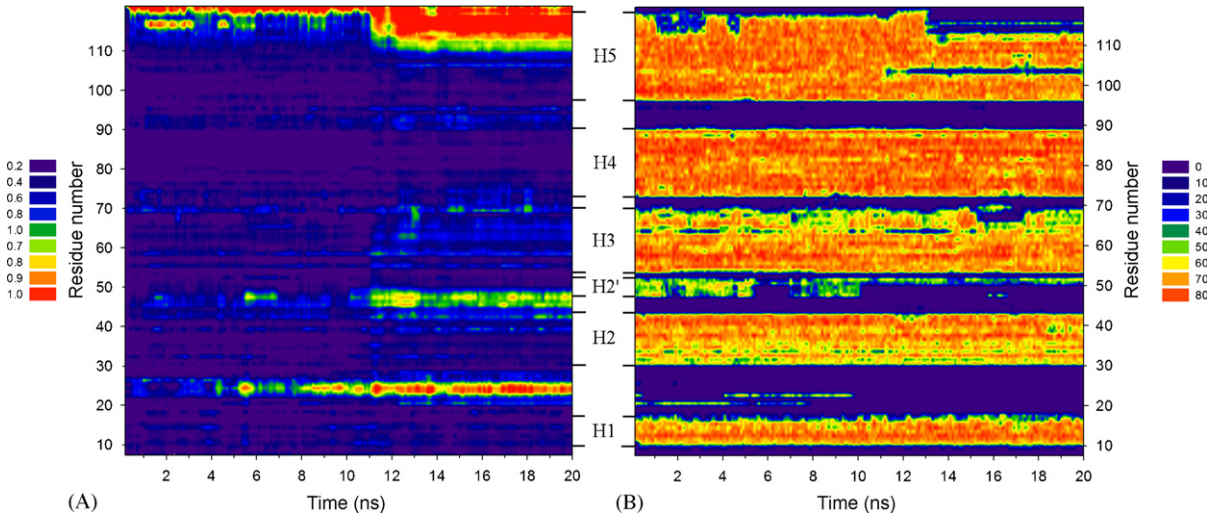

Fig. 4. (A) All-atom RMSD (in nm) from crystal structure, as a function of both residue number and time; (B) ellipticity at 222 nm (in %, the percent of time in which the residue present a helical character) [28], as a function of both residue number and time.

distorted during MD is the C-terminal portion of H5, where a sequence of at least eight amino acids residues is responsible for a deviation of about 0.9 nm from the crystal structure. Other regions, including the loops connecting H1 to H2 and H2 to H2′ also presented an important deviation from the reference structure.

Such deviations are originated in the helical content of p17, as can be observed from the ellipticity fluctuation [28] (Fig. 4B). After the first 10 ns an increase in the flexibility at H5 C-terminal portion can be clearly observed and, consequently, a lost of its helical character. At the end of simulation, H5 is two turns shorter and changed its conformation from X-ray towards the NMR described conformation (Fig. 1).

Additional modifications in p17 secondary structure during the trajectory could be observed in its small 3_{10} helixes. As shown in Fig. 4B, H2′ appears to be quite unstable, being completely lost after 10 ns of the MD simulation. Conversely, H3′ appears to refold into a α-helix and to merge with H3 (Fig. 4B) indicating that, while possibly involved in conformational changes during viral assembly, such structure is highly flexible (Fig. 4A) and could co-exist in multiple conformational states in solution. These observations corroborate the move from the X-ray structure to the NMR determined conformation of p17 and are summarized in Fig. 1.

3.3. NMR versus X-ray structures of p17

Based on the simulation presented here, it appears that some features of p17 X-ray structure are not stable under solution conditions. These results were obtained in a 20 ns MD simulation and reproduced in two other simulations of 10 ns each, in a total sampling of 40 ns. It is also important to note that these results are independent on the elected method for calculating the long-range electrostatic forces, since one of the 10 ns simulations was done with PME and the other with GRF. This agrees well with previous data indicating that these two methods yield similar results, both consistent with experimental data [29].

In order to obtain a robust description of the secondary structure of p17 in crystal and solution environments we used distinct methods (i.e. DSSP [16], STRIDE [17], and ellipticity [28]) to evaluate the protein conformational changes as a function of medium (Fig. 1). While all these methods agree well in the description of p17 secondary structure, through comparison of NMR (2TAM and 2HMX) and X-ray (1HIW) derived structures some important differences can be pointed: (1) the presence of very small β-strands in the loop connecting H1 and H2 in solution and its absence in the crystal; (2) the presence of two 3_{10} helix in crystal and its absence in solution (see further in the text); (3) partial unfolding of H5 in solution regarded to the crystal conformation.

The occurrence of small β-strands in p17 appears to be a solvent induced effect, since it does not appear in the p17 X-ray structure. Its absence in the performed MD simulations (by refolding from crystallographic structure) can be explained by the time scale required for the formation of β-turns (in the order of hundreds of nanoseconds) [30,31].

Regarded to the occurrence of 3_{10} helixes in p17 from both crystallographic and NMR data, we were not able to confirm the occurrence of H3′ in the NMR derived forms of p17, despite of the information given in a previous work where the deviation of such helix was shown when comparing the two methods of protein structure determination [6]. As the β-strands appear to be induced by solvent, the 3_{10} helixes in p17 seem to be stabilized in the crystal environment, since it occurs only in the X-ray determined structure. For instance: regarding to H2′, the residue Glu52 (chain A) perform long-range electrostatic interactions with Arg58 (chain Q), while two water mediated hydrogen bond networks occurs, the first one involving Asn47 (chain B), water 913 and Glu73 (chain A), and the second one around Glu52 (chain B), water 910 and Ser38 (chain B). Regarding to H3′, there is a hydrogen bond between Gln69 (chain A) and Gln59 (chain B), an

electrostatic interaction between Gln59 and Gln108 (both at chain A), and equivalent interactions considering the chains B and C. So these short helix structures appear to be induced by the interaction between p17 monomers, as those occurring in trimeric biological unit or as a crystal unit. In addition, the observation of Fig. 4A and B shows an increase in the flexibility of the loop connecting H2 to H2′ that well corroborates the lost of this 3_{10} helix.

Moreover, the most distinguishing feature when comparing X-ray and NMR solved conformations of p17 is the folding of H5. This helix changes to a random coil in solution, with a lost in helical character from up to 15 residues (Fig. 1). Indeed, MD simulation of crystal structure almost completely converts the X-ray structure of p17 to its NMR conformation, with the unfolding of the C-terminal of H5 plus H2′. Such change in the protein's secondary structure was confirmed by several algorithms, like DSSP and STRIDE. The molecular basis for such process appears to be, as mentioned above for the 3_{10} helixes, a series of crystallographic contacts, including: long-range electrostatic interactions between Asp121 (chain A) and Lys26 (chain B), electrostatic interactions between Gln116 (chain A) and Ala118 (chain C), a hydrogen bond between Lys114 (chain A) and backbone of Gly11 (chain Q), and a series of contacts with the neighbor chain R. These interactions include a great surface of hydrophobic and electrostatic contacts formed by both backbone and side chains of residues Asp96, Lys98, Glu99, Asp102, Lys103, Glu106, Asn109, Lys110, Lys113, and Lys114 from chain A and Pro23, Gly24, Gly25, Asp96, Lys98, Glu99, Asp102, Glu106, Asn109, and Lys110 from chain R (Fig. 5).

In the MD simulations presented here the chain A was isolated from the ABCQRS hexamer that constitutes the p17 structure in 1HIW crystal. As a consequence, this mosaic of interchain interactions is eliminated, and so are the forces that modulate H5 conformation (and the 3_{10} helixes) in the crystal. Instead of crystallographic interactions, new contacts were created with water molecules upon the addition of solvent, inducing conformational modifications in p17, as indicated by RMSD, radius of gyration, solvent-accessible surface, PROCHECK, DSSP, STRIDE, and ellipticity.

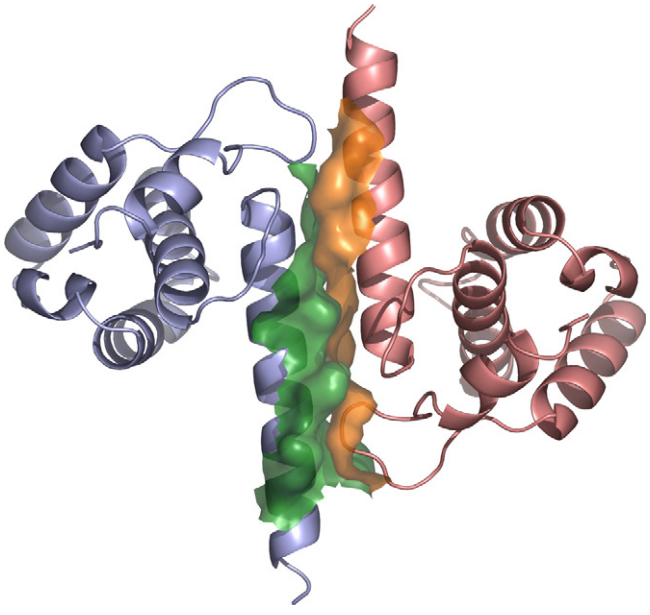

Fig. 5. Surface around intermolecular contacts between chains A (light blue and green) and R (pink and orange) of the 1HIW crystal structure.

A recent work reported the structure of the myristylated form of HIV-1 matrix protein using NMR method (PDB ID 1UPH [9]). While a preliminary observation of specific conformations indicates a full-folded α-helical H5 between residues Thr97 and Asp121, the full ensemble suggest a not well-defined C-terminal, which agrees with the MD results, as well as with previous NMR data of non-myristylated p17 [2,4].

In the view of the trimeric organization of HIV-1 matrix protein [5,3,7,10,11], we also performed MD simulations on this oligomeric form of p17. The obtained results confirm the progressive unfolding of H3′ (and its union with H3) and H5 in aqueous solutions (Fig. 1), indicating that the conformational modifications of this protein upon MD are not an artifact from the use of p17 monomeric form, but a direct consequence of solvent effects. As a consequence, such conformational changes are also expected to occur in trimeric forms of p17.

3.4. Implications to viral assembly

The HIV-1 matrix protein is a structural protein involved in different steps of the retrovirus life cycle, with different oligomerization states. As a monomer, it has a function in the early stages of virus replication and participates in the preintegration of the DNA complex into the nucleus of host cells [32], is involved in viral RNA binding [33] and transport to the plasma membrane [34]. Such roles of p17 depend on intermolecular interactions that, conversely, are determined by its solution conformation.

As a trimeric protein, the HIV-1 matrix protein has important function in incorporation of the HIV-1 envelope into virions [33], as well as in particle assembly [34]. It guides the binding of the precursor polyprotein, Gag, to the membrane through strong electrostatic and hydrophobic interactions [5,6,8–10]. While the electrostatic contribution comes from the N-terminal globular domain of p17, the hydrophobic contribution comes from the myristylation of the matrix protein [8]. However, little attention has been devoted on the C-terminal of H5. Considering the organization of matrix and capsid proteins [10], a direct interaction between the C-terminal of p17 should be expected to occur with the N-terminal end of p24 (Fig. 2A and B), guided by the trimeric p17. Such interaction will certainly depend on the conformation of the interacting proteins and, consequently, in the form adopted by the HIV-1 matrix protein in solution. Variations in p17 conformations would modify the energy associated with its interaction with p24 and, consequently, the viral compactness. Additionally, it appears that the partially unfolded form of H5 will be capable of a more efficient accommodation to the loops located in the upper face of p24 when compared to the completely folded one.

4. Conclusions

The comparison between macromolecules conformations obtained from different experimental proceedings can greatly contribute to the understanding of their biological functions at an atomic level. Most important, such comparison allows the isolation of conformational aspects dependent on the medium, i.e. solvent or crystal. However, the decision of which environment offers a better description of the protein conformation is not an easy task, as the bioactive conformation can be kept in the crystal and modified in a non-biological solution. On the other hand, the crystallographic medium is capable to induce conformational modifications in the protein, not observed in biological environment, but adequately described in solution conditions.

In this context MD simulations can greatly contribute to the understanding of the folding and structural patterns of macromolecules, as well as to the refinement of its structures/conformations through mimicking the biological environment expected to occur around them [27]. In the present work, we isolated the effects of crystal packing over the HIV-1 matrix protein, describing the conformation of p17 in aqueous solution. During the simulations the crystallographic conformation progressively changes to the NMR conformation, allowing the explanation for structural differences between crystal and solution conformations experimentally determined for p17.

The obtained results reinforce the use of MD simulations as an important tool to refinement of crystallographic derived structures. Moreover, it is our expectation that the described model of HIV-1 matrix protein can contribute to the understanding, at the atomic level, of the retrovirus life cycle and, consequently, to the structural role of its protein components.

Acknowledgements

This work was supported by Conselho Nacional de Desenvolvimento Científico e Tecnológico (CNPq), MCT, Brasília, Brazil; the Coordenação de Aperfeiçoamento de Pessoal de Nível Superior (CAPES), MEC, Brasília, Brazil; and Fundação de Amparo à Pesquisa do Estado do Rio Grande do Sul (FAPERGS), Porto Alegre, RS, Brazil.

References

[1] B.G. Turner, M.F. Summers, Structural biology of HIV, J. Mol. Biol. 285 (1999) 1–32.
[2] M.A. Massiah, M.R. Starich, C. Paschall, M.F. Summers, A.M. Christensen, W.I. Sundquist, Three-dimensional structure of the Human Immunodeficiency Virus type 1 matrix protein, J. Mol. Biol. 244 (1994) 198–223.
[3] M.V. Nermut, D.J. Hockley, J.B. Jowett, I.M. Jones, M. Garreau, D. Thomas, Fullerene-like organization of HIV gag-protein shell in virus-like particles produced by recombinant baculovirus, Virology 198 (1994) 288–296.
[4] S. Matthews, P. Barlow, N. Clark, S. Kingsman, A. Kingsman, I. Campbell, Refined solution structure of p17, the HIV matrix protein, Biochem. Soc. Trans. 23 (1995) 725–729.
[5] C.P. Hill, D. Worthylake, D.P. Bancroft, A.M. Christensen, W.I. Sundquist, Crystal structures of the trimeric human immunodeficiency virus type 1 matrix protein: implications for membrane association assembly, Proc. Natl. Acad. Sci. 93 (1996) 3099–3104.
[6] M.A. Massiah, D. Worthylake, A.M. Christensen, W.I. Sundquist, C.P. Hill, M.F. Summers, Comparison of the NMR and X-ray structures of the HIV-1 matrix protein: evidence for conformational changes during viral assembly, Prot. Sci. 5 (1996) 2391–2398.
[7] M.V. Nermut, D.J. Hockley, P. Bron, D. Thomas, W.H. Zhang, I.M. Jones, Further evidence for hexagonal organization of HIV gag protein in prebudding assemblies and immature virus-like particles, J. Struct. Biol. 123 (1998) 143–149.
[8] F. Bouamr, S. Scarlata, C. Carter, Role of myristylation in HIV-1 Gag assembly, Biochemistry 42 (2003) 6408–6417.
[9] C. Tang, E. Loeliger, P. Luncsford, I. Kinde, D. Beckett, M.F. Summers, Entropic switch regulates myristate exposure in the HIV-1 matrix protein, Proc. Natl. Acad. Sci. 101 (2004) 517–522.
[10] D. Huseby, R.L. Barklis, A. Alfadhli, E. Barklis, Assembly of human immunodeficiency virus precursor Gag proteins, J. Biol. Chem. 280 (2005) 17664–17670.
[11] M.J. Forster, B. Mulloy, M.V. Nermut, Molecular modeling study of p17gag (MA) protein shell utilizing data from electron microscopy and X-ray crystallography, J. Mol. Biol. 298 (2000) 841–857.
[12] C. Momany, L.C. Kovari, A.J. Prongay, W. Keller, R.K. Gitti, B.M. Lee, A.E. Gorbalenya, L. Tong, J. McClure, L.S. Ehrlich, M.F. Summers, C. Carter, M.G. Rossmann, Crystal structure of dimeric HIV-1 capsid protein, Nat. Struct. Biol. 3 (1996) 763–769.
[13] H.J.C. Berendsen, D. van der Spoel, R. van Drunen, GROMACS—a message-passing parallel molecular-dynamics implementation, Comput. Phys. Commun. 91 (1995) 43–56.
[14] D. van der Spoel, E. Lindahl, B. Hess, A.R. van Buuren, E. Apol, P.J. Meulenhoff, D.P. Tieleman, A.L.T.M. Sijbers, K.A. Feenstra, R. van Drunen, H.J.C. Berendsen, GROMACS User Manual Version 3.2, Nijenborgh 4, 9747 AG Groningen, The Netherlands, 2004.
[15] N. Guex, M.C. Peitsch, Swiss-model and the Swiss-Pdb Viewer: and environment for comparative protein modeling, Electrophoresis 18 (1997) 2714–2723. http://www.expasy.org/spdbv.
[16] W. Kabsch, C. Sander, Dictionary of protein secondary structure: pattern-recognition of hydrogen-bonded and geometrical features, Biopolymers 22 (1983) 2577–2637.
[17] D. Frishman, P. Argos, Knowledge-based protein secondary structure assignment, Proteins 23 (1995) 566–579.
[18] R.A. Laskowski, M.W. MacArthur, D.S. Moss, J.M. Thornton, PROCHECK: a program to check the stereochemical quality of protein structures, J. Appl. Crystallogr. 26 (1993) 283–291.
[19] W.L. DeLano, The PyMOL Molecular Graphics System, DeLano Scientific, Sao Carlos, CA, USA, 2002 http://www.pymol.org.
[20] H.J.C. Berendsen, J.P.M. Postma, W. van Gunsteren, J. Hermans, Interaction models for water in relation to protein hydration, in: B. Pullman (Ed.), Intermolecular Forces, Reidel, Dordrecht, The Netherlands, 1981, pp. 331–342.
[21] B.L. de Groot, H. Grubmüller, Water permeation across biological membranes: mechanism and dynamics of aquaporin-1 and GlpF, Science 294 (2001) 2353–2357.
[22] B. Hess, H. Bekker, H.J.C. Berendsen, J.G.E.M. Fraaije, LINCS: a linear constraint solver for molecular simulations, J. Comput. Chem. 18 (1997) 1463–1472.
[23] S. Miyamoto, P.A. Kollman, SETTLE: an analytical version of the SHAKE and RATTLE algorithm for rigid water models, J. Comput. Chem. 13 (1992) 952–962.
[24] T. Darden, D. York, L. Pedersen, Particle mesh Ewald—an $N \log(N)$ method for Ewald sums in large systems, J. Chem. Phys. 98 (1993) 10089–10092.
[25] I.G. Tironi, R. Sperb, P.E. Smith, W.F. van Gunsteren, A generalized reaction field method for molecular dynamics simulations, J. Chem. Phys. 102 (1995) 5451–5459.
[26] H.J.C. Berendsen, J.P.M. Postma, A. DiNola, J.R. Haak, Molecular-dynamics with coupling to an external bath, J. Chem. Phys. 81 (1984) 3684–3690.

[27] H. Verli, J.A. Guimarães, Insights into the induced fit mechanism in antithrombin–heparin interaction using molecular dynamics simulations, J. Mol. Graph. Mod. 24 (2005) 203–212.
[28] J.D. Hirst, C.L. Brooks III, Helicity, circular dichroism and molecular dynamics of proteins, J. Mol. Biol. 243 (1994) 173–178.
[29] A. Baumketner, J.-E. Shea, The influence of different treatments of electrostatic interactions on the thermodynamics of folding peptides, J. Phys. Chem. B 109 (2005) 21322–21328.
[30] W.A. Eaton, V. Munoz, P.A. Thompson, E.R. Henry, J. Hofrichter, Kinetics and dynamics of loops, α-helices, β-hairpins, and fast-folding proteins, Acc. Chem. Res. 31 (1998) 745–753.
[31] C.D. Snow, H. Nguyen, V.S. Pande, M. Gruebele, Absolute comparison of simulated and experimental protein-folding dynamics, Nature 420 (2002) 102–106.
[32] M.I. Bukrinsky, S. Haggerty, M.P. Dempsey, N. Sharova, A. Adzhubel, L. Spitz, P. Lewis, D. Goldfarb, M. Emerman, M. Stevenson, A nuclear localization signal within HIV-1 matrix protein that governs infection of non-dividing cells, Nature 365 (1993) 666–669.
[33] D. Trono, HIV accessory proteins: leading roles for the supporting cast, Cell 82 (1995) 189–192.
[34] P. Spearman, J.J. Wang, N. Van der Heyden, L. Ratner, Identification of human immunodeficiency virus type 1 Gag protein domains essential to membrane binding and particle assembly, J. Virol. 68 (1994) 3232–3242.
[35] F. Eisenhaber, P. Lijnzaad, P. Argos, C. Sander, M. Scharf, The double cube lattice method: efficient approaches to numerical integration of surface area and volume and to dot surface contouring of molecular assemblies, J. Comp. Chem. 16 (1995) 273–284.